

ASSESSMENT OF CREEP CRACK GROWTH DUE TO SECONDARY AND COMBINED LOADING

Priyesh Kapadia¹, Catrin M. Davies², David W. Dean³, and Kamran M. Nikbin⁴

¹ Research Engineer, Imperial College London, UK

² Lecturer, Imperial College London, UK

³ Chairman R5 Panel, EDF Energy, UK

⁴ Professor of Structural Integrity, Imperial College London, UK

ABSTRACT

The UK's advanced gas-cooled reactor power plants have welded components which were not stress relieved following fabrication. The presence of the weld induced residual stresses in combination with the low creep ductility of some heat affected zone material's has caused cracks to form during service at high temperature, due to a process known as reheat cracking.

An improved methodology to assess crack growth under combined loading conditions was published in a recent revision of the R5 high temperature structural integrity procedure. To validate this method, two novel fracture mechanics specimens were developed and used to perform crack growth studies, under secondary and combined loading conditions, in a laboratory controlled environment. Such test samples were produced by the insertion of wedges inside the mouths of C(T) specimens and by strategically placing electron beam welds in C(T) specimens such that the weld induced residual stresses caused crack growth.

Creep crack growth tests were conducted under secondary and combined loading conditions, at 550°C for up to 1,300 h, on specimens made of Type 316H stainless steel. The accumulation of creep strains, during relaxation of the residual stresses, caused crack growth of up to ≈ 5 mm to occur. The experimentally measured crack extensions were compared to predictions made using the new R5 approach. The crack growth estimates were found to be consistent with experimental measurements. Through sensitivity studies the conservatism in the assessment procedure are presented.

INTRODUCTION

Steel components used within advanced gas-cooled reactor (AGR) power plants operating in the UK have welded components which were not post weld heat treated following fabrication. The misfit of the plastically deformed welded region and surrounding parent material causes elastic strains, and therefore induces residual stresses in such components. During operation at high temperature creep strains accumulate to reduce the magnitude of these elastic strains. Hence the effect of the misfit is reduced and the residual stresses relax. In low creep ductility materials, the accumulation of these creep strains can lead to creep damage in the form of intergranular voids and can eventually cause crack formation. Creep crack growth (CCG) due to residual stresses is known as reheat cracking. Reheat cracking has been observed in-service in AGR power plants, where cracks have been observed in non stress relieved AISI Type 316H stainless steel components (Coleman Miller, D. A. and Stevens, R. A., 1998).

Estimates of crack growth may be made using the R5 high temperature structural integrity procedure (EDF Energy, 2014). The latest revision contains an improved methodology to estimate crack growth using the creep fracture mechanics parameter $C(t)$, which is determined using a reference stress approach. In such assessment procedures, the crack tip stresses are categorised as primary or secondary. Secondary stresses are those which do not contribute to plastic collapse and arise to accommodate a strain mismatch which

could be induced from local distortions or thermal gradients. Secondary stresses are self-equilibrating across the structure and at high temperature tend to relax due to creep deformation. Primary stresses are generated by applied loads such as bending or pressure which could lead to plastic collapse of the structure. Combined loading conditions occur where both primary and secondary stresses exist. Appendix A3 of R5 Volume 4/5 contains a procedure to determine $C(t)$ under combined loading conditions, which is investigated in this paper.

Assessment procedures need to be experimentally validated with tests performed under controlled conditions, to demonstrate that they provide accurate and conservative crack growth predictions. To facilitate this, two novel creep crack growth (CCG) test specimens have been developed, where residual stresses were induced in compact tension, C(T), specimens. These allowed CCG tests to be performed under secondary and combined loading. A summary of the specimen designs and test results is presented in the following section with further detail in (Kapadia et al., 2015). In this paper, the experimentally observed crack lengths are compared to predictions made using the methodology presented in Appendix A3 of R5 Volume 4/5.

EXPERIMENTAL TESTS

CCG testing was performed using two specimen designs which are shown in Figure 1. Residual stresses were induced in the wedge-loaded C(T) specimens by insertion of wedges into the mouths of C(T) specimens which had a tapered mouth profile. The wedges were held in place due to the compressive load from the modified C(T) specimens and friction. C(T) specimens were also fabricated from blocks containing electron beam (EB) welds. In the wedge-loaded and EB welded C(T) specimens, residual stresses were induced by the geometrical misfits of the oversized wedge and by the plastically deformed region surrounding the EB weld respectively.

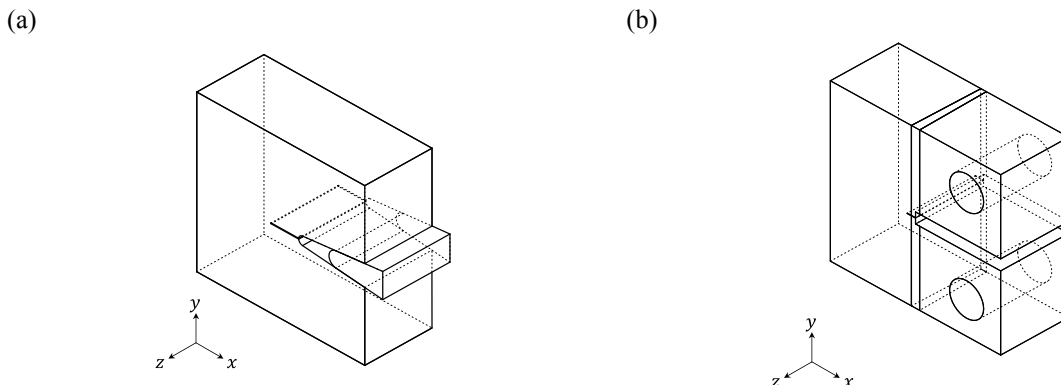


Figure 1. (a) Wedge-loaded C(T) specimen and (b) EB welded C(T) specimen.

Specimens were made using ex-service Type 316H stainless steel which was pre-conditioned to reduce the material's creep ductility. C(T) blanks were uniformly pre-compressed to 8% plastic strain before fabrication into the C(T) specimens. This process reduced the creep ductility to increase the likelihood of crack growth would occur during subsequent CCG testing (Mehmanparast et al., 2013). In similar studies where CCG tests were conducted under secondary loading, only limited crack growth occurred (Hossain, Truman, & Smith, 2011; Yazdani, 2012). This is likely to have been due to the relatively higher creep ductility of the ex-service Type 316H stainless steel which was in the as-received condition.

The wedge-loaded C(T) specimens were tested with three different wedge insertion depths such that tests were conducted with three magnitudes of crack driving force, which is quantified by the stress intensity

factor due to secondary loading, K^S . The wedge-loaded C(T) specimen could only be used to test under secondary loading conditions as any applied load would oppose the effect of the wedge. Hence the EB welded specimens were used to conduct tests under secondary and combined loading conditions. The crack driving force due to the primary and secondary loads characterised by the parameter K^P and K^S respectively are shown in Table 1. Specimens were tested at 550°C for test durations of t_T hours, as shown in Table 1. The maximum crack extensions, Δa_{max} , observed which were at mid thickness of the specimens are also shown in Table 1. Further detail of the crack profile are presented in (Kapadia et al., 2015).

Table 1. CCG test specimens with residual stresses showing crack driving forces and crack extensions

Specimen	t_T (h)	K^P (MPam ^{1/2})	K^S (MPam ^{1/2})	Δa_{max} (mm)
WC(T)3	329	0.0	36.0	0.9
WC(T)4	329	0.0	43.6	1.8
WC(T)5	885	0.0	40.4	5.4
EBW3	1,320	0.0	16.0	0.0
EBW5	1,340	0.0	22.2	1.2
EBW6	1,300	5.0	22.2	3.1
EBW7	1,320	10.0	22.2	3.3

CRACK GROWTH PREDICTIONS USING THE R5 PROCEDURE

C(t) Definition in the R5 Procedure

The stresses around a crack tip in a material deforming under steady state creep conditions are constant and may be defined using the parameter C^* which defines the magnitude of the stress field. At short times, transient conditions exist where the magnitude of the stress field is time dependent and is described by the parameter $C(t)$. Where residual stresses are present, stress relaxation occurs and transient creep conditions exist, therefore the magnitude of the stress field must be described using $C(t)$.

In the R5 procedure, the parameter $C(t)$ is determined using the reference stress, σ_{ref} . The reference stress is a measure of proximity to plastic collapse and for primary loading is defined by:

$$\sigma_{ref}^p = \frac{P}{P_{LC}} \sigma_y \quad (1)$$

where P is the applied load and P_{LC} is the load that causes plastic collapse of the component. For a C(T) specimen P_{LC} is given in R6 Section IV.1.9.1 (EDF Energy, 2015).

Appendix A3 of R5 Volume 4/5 presents a solution for $C(t)$ under combined loading. For small amounts of crack growth, $C(t)$ is estimated in a material which exhibits power law creep by:

$$\frac{C(t)}{C^*} = \frac{\sigma_{ref} \dot{\epsilon}_{ref}}{\sigma_{ref}^p \dot{\epsilon}_{ref}^p} \left[\frac{(\epsilon_{ref}/\epsilon_{ref}^0)^{n+1}}{\phi(t) \left[(\epsilon_{ref}/\epsilon_{ref}^0)^{n+1} - 1 \right] + (1 - \sigma_{ref}^0/E\epsilon_{ref}^0)} \right] \quad (2)$$

where ϵ_{ref} is the total reference strain, ϵ_{ref}^0 is the initial reference strain, $\dot{\epsilon}_{ref}$ is the reference creep strain rate and n is the creep exponent. The strain ϵ_{ref} includes elastic, plastic and creep deformations. The parameter C^* is included in the expression as a normalising parameter and is defined by:

$$C^* = \sigma_{ref}^p \dot{\epsilon}_{ref}^p R' \quad (3)$$

where $\dot{\varepsilon}_{ref}^p$ is the reference creep strain rate due to primary loads only and R' is a characteristic length defined by:

$$R' = \left(\frac{K^p}{\sigma_{ref}^p} \right)^2 \quad (4)$$

Under secondary loading conditions alone, $C^* = 0$ and hence cannot be used to normalise $C(t)$ in Equation (2). Hence $C(t)$ is normalised by C_0^* which is the steady state value of C^* that would exist if the initial residual stress was induced by a primary load that does not relax (Lei, 2013):

$$C_0^* = \sigma_{ref}^0 \dot{\varepsilon}_{ref}^0 R' \quad (5)$$

Therefore:

$$\frac{C(t)}{C_0^*} = \frac{\sigma_{ref} \dot{\varepsilon}_{ref}}{\sigma_{ref}^p \dot{\varepsilon}_{ref}^p} \left[\frac{(\varepsilon_{ref}/\varepsilon_{ref}^0)^{n+1}}{\phi(t) \left[(\varepsilon_{ref}/\varepsilon_{ref}^0)^{n+1} - 1 \right] + (1 - \sigma_{ref}^0/E\varepsilon_{ref}^0)} \right] \quad (6)$$

which may be used for both secondary and combined loading conditions. The normalisation approach does not change the estimate of $C(t)$.

In Equation (6) the parameter ϕ is a time dependent function of the elastic follow up factor, Z and has a value $1 \leq \phi(t) \leq Z/(Z - 1)$. R5 Volume 4/5 Appendix A3 (Section A3.4.3.3) recommends a conservative estimate of $\phi(t) = 1.0$ may be taken.

Under elastic-creep conditions Equation (6) reduces to:

$$\frac{C(t)}{C_0^*} = \frac{\sigma_{ref} \dot{\varepsilon}_{ref}}{\sigma_{ref}^p \dot{\varepsilon}_{ref}^p} \left[\frac{(E\varepsilon_{ref}/\sigma_{ref}^0)^{n+1}}{\phi(t)(E\varepsilon_{ref}/\sigma_{ref}^0)^{n+1} - 1} \right] \quad (7)$$

Determining the Relaxation of Reference Stresses under Secondary and Combined Loading

For combined loading the initial reference stress, σ_{ref}^0 , in R5 Volume 4/5 Appendix A3 (Section A3.4.1.1) Method 1 may be determined from K^p and K^s by Equation (8), however using the advice in R6 Section II.6, this may also be expressed as Equation (9) which is equivalent (EDF Energy, 2015; Lei, 2013).

$$\sigma_{ref}^0 \varepsilon_{ref}^0 = \frac{(\sigma_{ref}^p)^2 (1 + V K^s/K^p)^2}{E f^2(L_r)} \quad (8)$$

$$\sigma_{ref}^0 \varepsilon_{ref}^0 = \frac{(\sigma_{ref}^p + \xi K_j^s/\sqrt{R'})^2}{E f^2(L_r)} \quad (9)$$

where the parameter V defines the interaction between the primary and secondary stress and $f(L_r)$ is the failure assessment curve which are defined in R6. Equation (9) is more convenient to solve for secondary loading conditions and uses the effective stress intensity factor for secondary loads, K_j^s , which is determined from the J -integral. For secondary loads only, K^s is equal to K_j^s in accordance with R6 Section 11.6.4.2.

The parameter ξ is a constant determined from V and is tabulated in R6 Table II.6.3. For secondary loads only $L_r = 0$ and due to this, $\xi = 1$ and $f(L_r) = 1$.

The parameter R' is defined by Equation (4). As both K^p and σ_{ref}^p are a function of the applied load, P , the parameter R' may still be determined for secondary loading where $P = 0$. However, this approach assumes the stress distribution defined by K^p and σ_{ref}^p are representative of that produced by the residual stresses.

The stress relaxation rate under combined loading conditions is defined in R5 as:

$$\dot{\sigma}_{ref} = -\frac{E}{Z} \left(\dot{\varepsilon}_c(\sigma_{ref}) - \dot{\varepsilon}_c(\sigma_{ref}^p) \right) \quad (10)$$

where $\dot{\varepsilon}_c$ is the creep strain rate determined at the total reference stress, σ_{ref} , or the primary reference stress, σ_{ref}^p . The reference strain is defined in R5 Volume 4/5 Appendix A3 as:

$$\varepsilon_{ref} = \varepsilon_{ref}^0 - \frac{\sigma_{ref}^0 - \sigma_{ref}}{E} + \varepsilon_{ref}^c \quad (11)$$

where ε_{ref}^0 is the initial reference strain and ε_{ref}^c is the reference creep strain. The first term, ε_{ref}^0 , includes elastic and plastic strains, and the second term defines the reduction in elastic strain during stress relaxation. In this definition the plastic contribution of the initial reference strain remains throughout stress relaxation. Estimates of ε_{ref}^0 may be made using a material's stress-strain curve or a constitutive model such as the Ramberg-Osgood model.

Material Properties

The elastic strains were determined using the Young's modulus of the material at 550°C which was experimentally determined as 140 GPa (Mehmanparast et al., 2013). The plastic strains were determined using the Ramberg-Osgood material model:

$$\varepsilon = \frac{\sigma}{E} + A\sigma^N \quad (12)$$

where E is Young's modulus and, A and N are constants that are fitted to experimental uniaxial tensile test data. The constants A and N were fitted to tensile test data at 550°C for pre-compressed Type 316H stainless steel (Mehmanparast et al., 2013), and were determined as 2.56×10^{-21} and 7.45 respectively (for σ in MPa and ε in mm/mm).

The Norton law was used to define the creep properties of the material where an average creep strain rate was assumed. The average creep strain rate, $\dot{\varepsilon}_A^c$, is defined as the ratio of the uniaxial failure strain, ε_f , to the rupture time in a uniaxial creep test, t_r :

$$\dot{\varepsilon}_A^c = \frac{\varepsilon_f}{t_r} = C\sigma^n \quad (13)$$

where C and n are temperature dependent material constants. For Type 316H stainless steel, this law was empirically fitted to test data from 87 constant-load creep tests conducted at 550°C (Webster et al., 2008). The constants C and n were determined as 1.05×10^{-25} and 8.45 respectively, (for ε^c in mm/mm, σ in MPa and t in units of h respectively).

C(t) in Wedge-Loaded and EB Welded C(T) Specimens

The initial reference stresses for the wedge-loaded and EB welded C(T) specimens were determined using Equations (9) and are shown in Table 2. The reference stresses are greater in the wedge-loaded C(T) specimens which have large K^S . All values of σ_{ref} are significantly less than the material's yield strength at 550°C, which is 259 MPa (Mehmanparast et al., 2013).

Equation (10) was evaluated to determine relaxation of σ_{ref}^0 , and was numerically integrated using the Runge Kutta method. An elastic follow up factor of $Z = 3.0$ was assumed for all specimens. From σ_{ref} , the creep fracture mechanics parameter, $C(t)$, was determined for the wedge-loaded and EB welded C(T) specimens and its variation with time is shown in Figure 2. At short times, $C(t)$ values determined using elastic-plastic-creep properties are less than those determined using elastic-creep properties. Plasticity reduces the magnitude of crack tip stresses and hence the values of $C(t)$ are smaller. At longer times, $C(t)$ values determined using material properties with and without plasticity converge to the same magnitude. In general the magnitude of $C(t)$ reduces for all specimens as the residual stresses relax.

Table 2. Reference stress estimates for C(T) specimens with secondary and combined loads.

Specimen	K^S (MPam ^{1/2})	K^P (MPam ^{1/2})	σ_{ref}^p (MPa)	L_r	R' (mm)	ξ	σ_{ref}^0 (MPa)
WC(T)3	36.0	0.0	0.0	0.00	94.2	1.000	117.3
WC(T)4	43.6	0.0	0.0	0.00	96.0	1.000	140.7
WC(T)5	40.4	0.0	0.0	0.00	95.1	1.000	131.0
EBW5	22.2	0.0	0.0	0.00	94.1	1.000	71.7
EBW6	22.2	5.0	16.3	0.06	94.1	1.009	88.6
EBW7	22.2	10.0	32.6	0.13	94.1	1.018	105.6

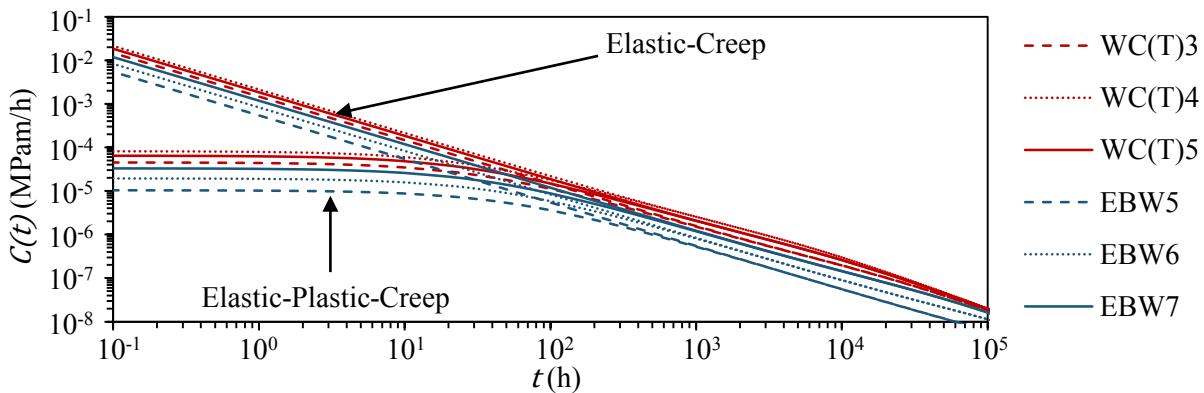


Figure 2. $C(t)$ determined during stress relaxation in the C(T) specimens assuming elastic-plastic creep and elastic-creep material properties.

Sensitivity Studies

The $C(t)$ values presented in Figure 2 were determined assuming an elastic follow up factor of $Z = 3.0$ for all specimens. Studies were performed to determine the sensitivity to the value of Z . Figure 3 shows $C(t)$ determined for specimen WC(T)5 for three values of Z . At small times the estimates of $C(t)$ values were insensitive to Z . At times larger than 1,000 hours $C(t)$ values were greater for large Z . Where elastic follow up is significant, the rate of stress relax slowly and hence the magnitude of the stress field surrounding a crack tip remains large.

True stress vs. plastic strain measurements made on 8% pre-compressed Type 316H stainless steel are shown in Figure 4(a), data from (Mehmanparast et al., 2013). The constants for the Ramberg-Osgood model, A and N , were fitted up to $\varepsilon^{pl} = 10\%$ and determined as 2.56×10^{-21} and 7.45 respectively for this study. However Mehmanparast et al. fitted the Ramberg-Osgood model to the entire stress-strain curve, where A and N were determined as 5.11×10^{-15} and 5.00 respectively. For specimen WC(T)5, where $\sigma_{ref}^0 = 131.0$ MPa, the initial plastic strain was determined as 197 $\mu\varepsilon$ and 15 $\mu\varepsilon$ for the Ramberg-Osgood model fitted to failure and fitted up to $\varepsilon^{pl} = 10\%$ respectively. Estimates of $C(t)$ for each of these deformation models and in the limiting case of no plasticity, for specimen WC(T)5, are shown in Figure 4(b). The $C(t)$ estimates at short times are very sensitive to ε^{pl} and therefore the plasticity model assumed. The Ramberg-Osgood model determines plastic strains at all stresses, i.e. no limit of proportionality is included in the law. As σ_{ref}^0 values were low for all C(T) specimens tested in this study, the Ramberg-Osgood model fitted up to $\varepsilon^{pl} = 10\%$ was considered to give the most accurate predictions of plastic strains.

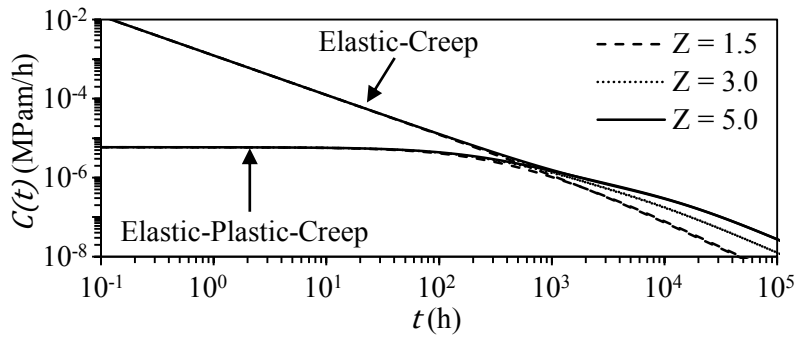


Figure 3. $C(t)$ determined during stress relaxation in the C(T) specimens assuming elastic-plastic creep and elastic-creep material properties.

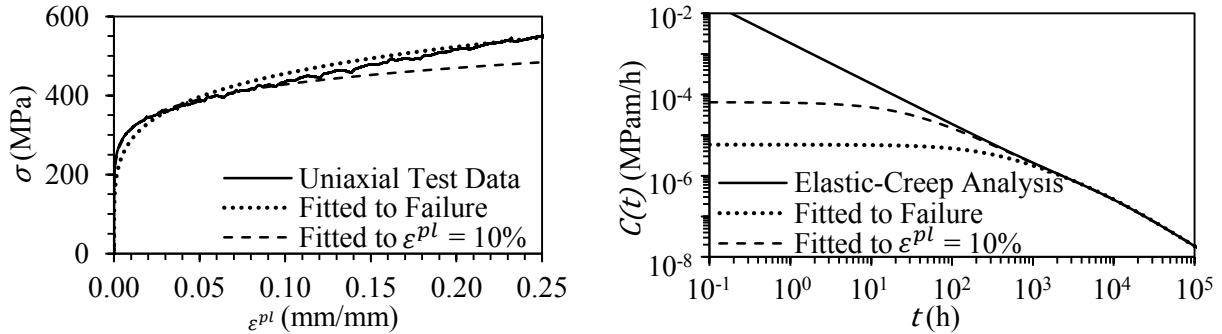


Figure 4. (a) True stress vs. plastic strain from uniaxial tensile test compared to Ramberg-Osgood models and (b) sensitivity of $C(t)$ estimation in WC(T)5 to plastic strain

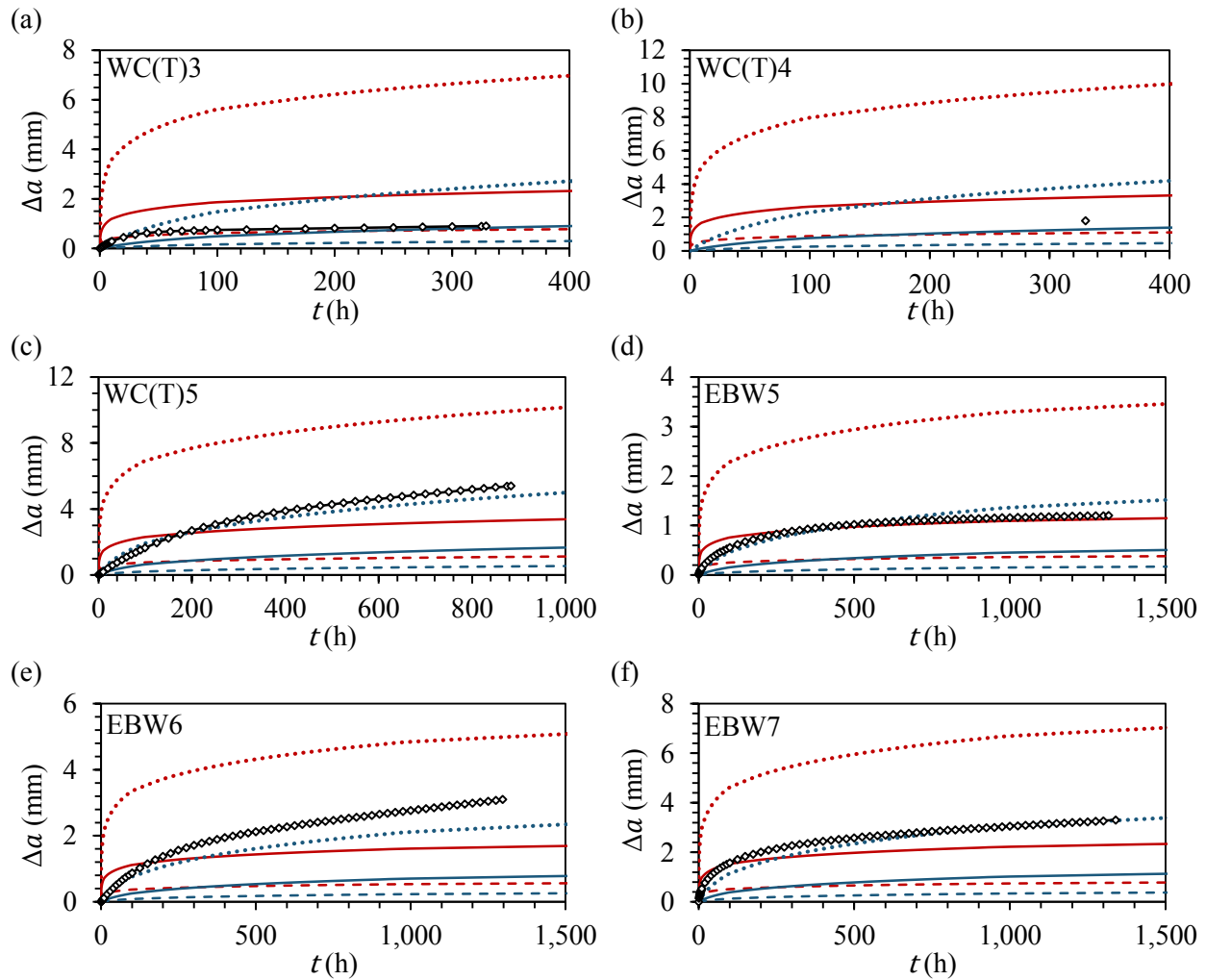
Estimates of CCG using the R5 Procedure

An expression to determine the crack growth rate, \dot{a} , is presented in R5 Volume 4/5:

$$\dot{a} = D (C(t))^\phi \quad (14)$$

where D and ϕ are material constants that can be determined empirically from experimental data. These constants were determined from CCG tests on 8% pre-compressed Type 316H stainless steel under primary

load conditions at 550°C (Mehmanparast et al., 2013), and were determined as 94 and 0.91 respectively, (for \dot{a} in mm/h and $C(t)$ in MPam/h). Due to large scatter in the CCG data, a multiplicative factor for the constant D was determined as 3.01 which estimates the upper bound (UB) and lower bound (LB) fits.



	CCG Properties			Test Data
	Upper Bound	Mean	Lower Bound	
Elastic-Creep	————	-----	—○—
Elastic-Plastic-Creep	————	-----	

Figure 5. Comparison of crack growth predictions from $C(t)$ with experimentally measured crack length in specimens: (a) WC(T)3, (b) WC(T)4, (c) WC(T)5, (d) EBW5, (e) EBW6 and (f) EBW7.

Estimates of crack growth in the C(T) specimens were made using Equation (14) with the $C(t)$ estimates shown in Figure 2, determined using elastic-creep and elastic-plastic-creep deformation assumptions. Crack extension predictions were made using the mean, upper and lower bound CCG properties, and are shown in Figure 5.

Crack length predictions made by assuming elastic-creep material properties and mean CCG properties provides a reasonable estimate of the experimental crack length. In specimens WC(T)3 and WC(T)4 the

assessment predicts a crack length of up to 1.5 mm greater than the experimental measurements, whilst in specimen EBW5 the predictions are in excellent agreement with the experimental measurements. However in specimens WC(T)5, EBW6 and EBW7 the assessment assuming elastic-creep properties and mean CCG data under-predicts the crack lengths by up to 2.1 mm. The upper and lower bounds represent the scatter in CCG rates observed in experimental testing under primary load conditions. Using the UB/LB fits, bounding crack lengths were estimated. The experimental crack length measurements lie within the UB/LB estimates where elastic-creep material properties are assumed. However for some of these specimens, UB crack length predictions are up to 10 times larger than experimental observations and therefore are overly conservative.

The crack extensions predicted assuming elastic-plastic-creep deformation were less than that assuming elastic-creep deformations, as shown in Figure 5, due to lower values of $C(t)$ at short times. The crack growth predictions assuming elastic-plastic-creep deformations and mean CCG properties were in close agreement with the experimental measurements in WC(T)3 and WC(T)4, whereas for specimen WC(T)5 and the EB welded specimens the crack length measurements were close to the upper bound predictions.

DISCUSSION

Crack growth predictions made using $C(t)$ determined from the R5 procedure, assuming limited crack growth were generally conservative. The extent of conservatism was dependent on whether elastic-creep or elastic-plastic-creep properties were assumed and also whether mean, upper or lower bound fits to the CCG properties were used. Crack growth predictions assuming elastic-creep deformation and using the UB CCG fit bounded all of the experimental results, however for some specimens were overly conservative. This was due to the large $C(t)$ estimated at short times which resulted in initially high crack growth rates. By including plasticity, the estimates of $C(t)$ at short times were reduced. However the predictions were sensitive to the accuracy of the plasticity model and for many of the specimens the initial crack growth rate was under-predicted by assuming elastic-plastic-creep deformation. When making assessments using the $C(t)$ estimation methodology presented in the R5 procedure, care must be taken that the extent of plasticity is not over-estimated as this could make the predictions non-conservative.

Crack growth predictions made using $C(t)$ estimates were sensitive to the CCG properties assumed. Specimen WC(T)5 had small grains in comparison to WC(T)3 and WC(T)4, as shown by (Kapadia et al., 2015). It was considered that this difference in microstructure contributed to a faster crack growth rate and hence the assessments using the UB crack growth fits provided more accurate predictions. In general the UB and LB predictions show a large spread in crack lengths which is typical of the material tested. Large differences in creep ductilities have been observed based on the cast and service history of the material (Chevalier, 2013; Webster et al., 2008). When making component lifetime assessments, the microstructure of a component is usually unknown. For conservatism, the UB $\dot{a} - C^*$ fit should be used to predict crack lengths but this can lead to very conservative crack growth estimates.

In the EB welded C(T) specimens, the experimental measurements were greater than predictions made assuming elastic-plastic-creep deformation and mean crack growth properties, and were close to the upper bound estimates. The experimental measurements were in good agreement to predictions made assuming elastic-creep deformation. In these specimens, up to 3% weld induced plastic strains existed ahead of the crack tip from EB welding, as shown by (Kapadia et al., 2015). Plasticity reduced the creep ductility of the material and hence this contributed to the increased crack growth rates measured in comparison to the predictions made using the CCG properties of material in the 8% pre-compressed condition. The presence of weld induced plasticity was not accounted for in the assessment. This supports the observations by (Turski et al., 2008) where the plasticity induced in the pre-compressed C(T) specimens influenced the crack growth rate. Further work is needed to develop the assessment approach to include the effect of prior plasticity on crack growth rates. This is important for carrying out lifetime assessments for components in

service, as reheat cracking is a concern in welded components where weld induced plasticity reduces the creep ductility of the material.

CONCLUSIONS

Creep testing was conducted in recently developed C(T) specimens with residual stresses, to investigate CCG under secondary and combined loading. In these tests cracks lengths of up to 5.4 mm were observed after up 1,300 hours of testing specimens made of pre-compressed Type 316H stainless steel at 550°C. Crack growth predictions were made using $C(t)$ estimated by following the approach in the latest revision of the R5 procedure, in combination with $\dot{a} - C^*$ trends that were published in the literature for CCG tests on the same material under primary loading conditions.

The analysis presented shows the crack growth estimates using the reference stress methodology in R5 Volume 4/5 Appendix A3 are in good agreement with the experimental data. It is shown that performing the assessment using elastic-creep deformation produces conservative crack growth estimates. However elastic-plastic-creep material properties provide more accurate predictions of $C(t)$ values at short times. Furthermore it is shown that upper bound crack growth properties can be used in assessments to take into account reduction in creep ductility which may be caused by plasticity or microstructure variability in the component.

REFERENCES

- Chevalier, M. (2013). *The Reliability of Degrading Structural Systems Operating at High Temperature*. University of Bristol, UK.
- Coleman Miller, D. A. and Stevens, R. A., M. C. (1998). "Reheat Cracking and Strategies to Assure Integrity of Type 316 Welded Components.," In *Integrity of High Temperature Welds*, 169–180. London: Professional Engineering Publishing Limited.
- EDF Energy. (2014). *R5: Assessment Procedure for the High Temperature Response of Structures*, Issue 3 Revision 001, Gloucester, UK.
- EDF Energy. (2015). *R6: Assessment of the Integrity of Structures Containing Defects*, Revision 4 with amendments to Amendment 11, Gloucester, UK.
- Hossain, S., Truman, C. E., & Smith, D. J. (2011). "Generation of residual stress and plastic strain in a fracture mechanics specimen to study the formation of creep damage in type 316 stainless steel.," *Fatigue & Fracture of Engineering Materials & Structures*, 34, 654–666.
- Kapadia, P., Davies, C. M., Dean, D. W., & Nikbin, K. M. (2015). "Creep Crack Growth Testing under Secondary and Combined Loading.," In *ASME 2015 Pressure Vessels & Piping Division Conference*, American Society of Mechanical Engineers.
- Lei, Y. (2013). *FE Creep Analysis of a Single-Edge-Cracked Plate under Combined Primary and Secondary Loading*, EDF Energy Report E/REP/BBGB/0056/GEN/09, Gloucester, UK.
- Mehmanparast, A., Davies, C. M., Dean, D. W., & Nikbin, K. M. (2013). "The influence of pre-compression on the creep deformation and failure behaviour of Type 316H stainless steel.," *Engineering Fracture Mechanics*, 110, 52–67.
- Turski, M., Bouchard, P. J., Steuwer, A., & Withers, P. J. (2008). "Residual stress driven creep cracking in AISI Type 316 stainless steel.," *Acta Materialia*, 56, 3598–3612.
- Webster, G. A., Davies, C. M., Skelton, R. P., & Nikbin, K. M. (2008). *Comparison of R5 Volume 4/5 Procedures for Determining Incubation Periods in Type 316H Stainless Steel*, ICON Report No. ME 115/01, Imperial College London, UK
- Yazdani, H. Y. (2012). *Effect of Prior Deformation on Creep Behaviour of AISI 316H Austenitic Stainless Steels*. Materials and Surface Science Institute, Department of Mechanical, Aeronautical and Biomedical Engineering. University of Limerick, Republic of Ireland.